Association and Dissociation of Lithium Cyanocuprates in Ethereal Solvents

*Aliaksei Putau and Konrad Koszinowski**

Department Chemie, Ludwig-Maximilians-Universität München, Butenandtstr. 5 – 13, 81377 München, Germany

Supporting Information

Table of Contents

1.) Additional negative ion mode ESI mass spectra of $LiCuR_2 \cdot LiCN$ solutions (Figures S1 – S8) **S2**

2.) Additional positive ion mode ESI mass spectra of $LiCuR_2 \cdot LiCN$ solutions (Figures S9 – S16) **S6**

3.) Additional negative ion mode ESI mass spectra of $Li_{0.8}CuR_{0.8}(CN)$ solutions (Figures S17 – S24) **S10**

4.) Additional positive ion mode ESI mass spectra of $Li_{0.8}CuR_{0.8}(CN)$ solutions (Figures S25 – S32) **S14**

5.) Concentration dependence of the molar conductivity of $LiCuPh_2 \cdot LiCN$ (Figure S33) **S18**

6.) Temperature dependence of the molar conductivity of LiCuPh(CN) (Figure S34) **S19**

1.) Additional negative ion mode ESI mass spectra of $LiCuR_2$·LiCN solutions

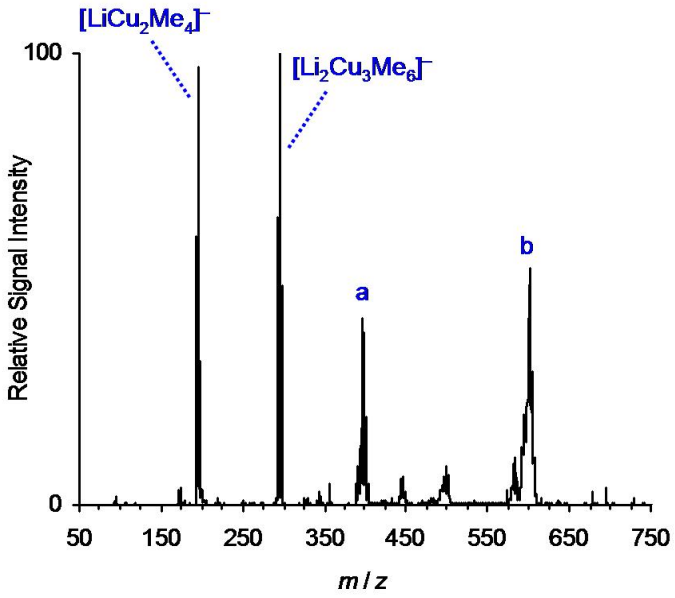

Figure S1. Negative ion mode ESI mass spectrum of a 25 mM solution of $LiCuMe_2$·LiCN in Et_2O, a = $Li_3Cu_4Me_{8-x}(OH)_x^-$, b = $Li_5Cu_6Me_{12-x}(OH)_x^-$, x = 1 – 3.

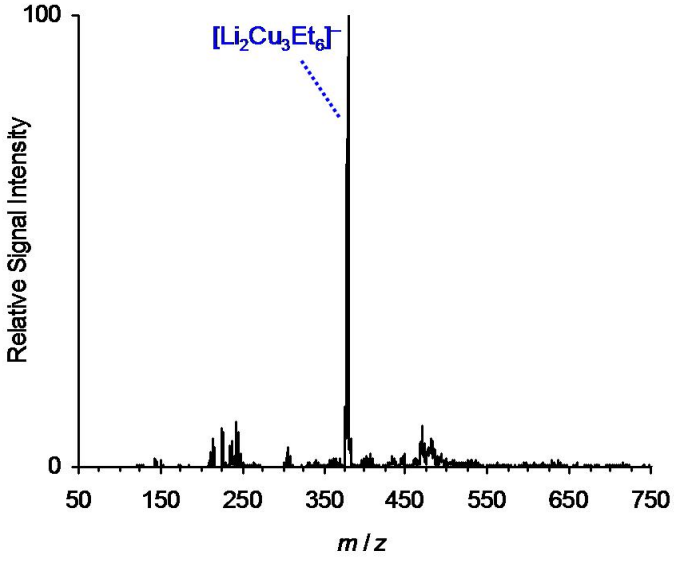

Figure S2. Negative ion mode ESI mass spectrum of a 25 mM solution of $LiCuEt_2$·LiCN in Et_2O.

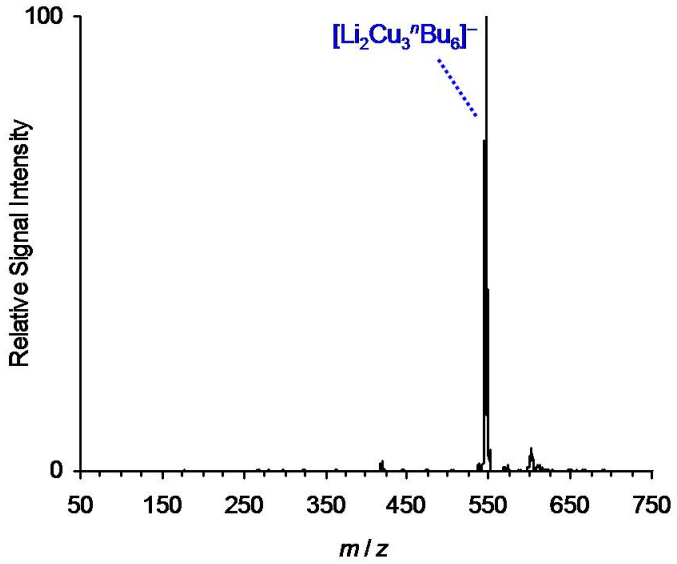

Figure S3. Negative ion mode ESI mass spectrum of a 25 mM solution of $LiCu^{n}Bu_2 \cdot LiCN$ in Et_2O.

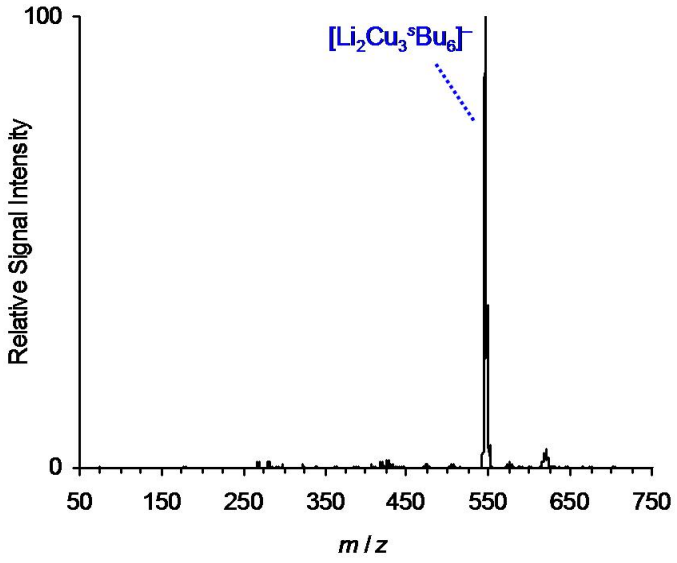

Figure S4. Negative ion mode ESI mass spectrum of a 25 mM solution of $LiCu^{s}Bu_2 \cdot LiCN$ in Et_2O.

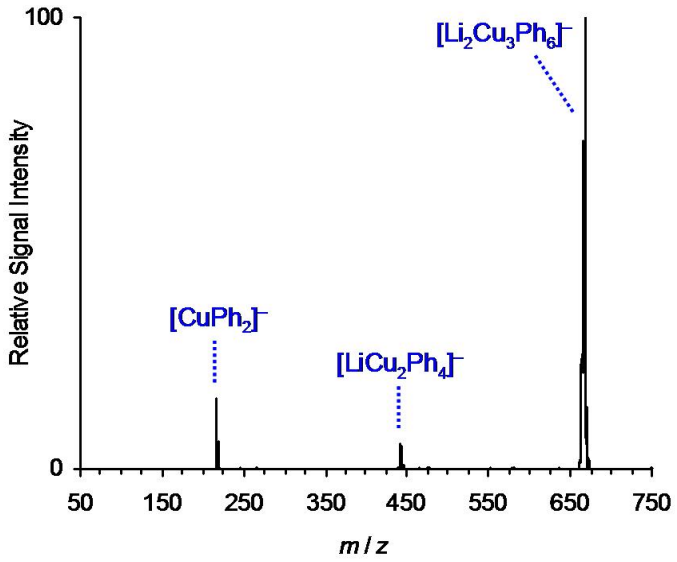

Figure S5. Negative ion mode ESI mass spectrum of a 25 mM solution of $LiCuPh_2 \cdot LiCN$ in Et_2O.

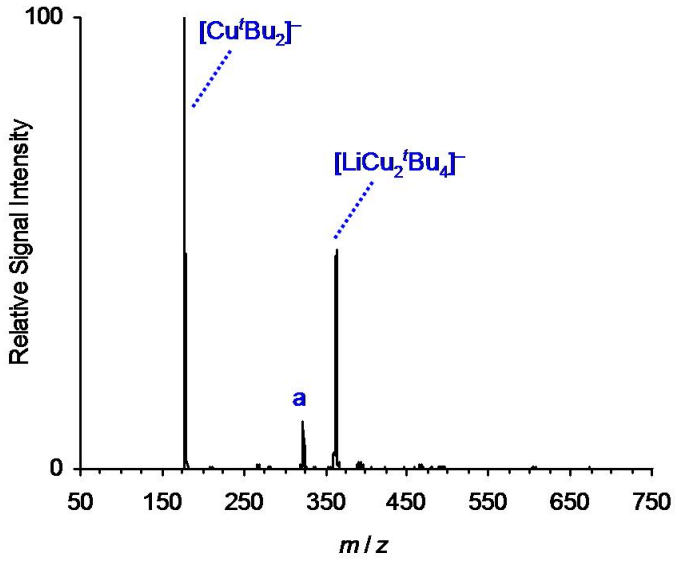

Figure S6. Negative ion mode ESI mass spectrum of a 25 mM solution of $LiCu^tBu_2 \cdot LiCN$ in MeTHF, a = $LiCu_2{}^tBu_3(OH)^-$.

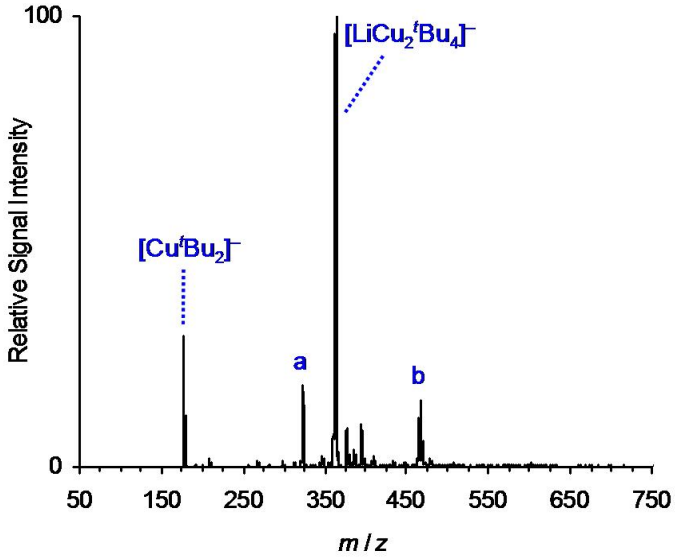

Figure S7. Negative ion mode ESI mass spectrum of a 25 mM solution of $LiCu^tBu_2 \cdot LiCN$ in CPME, a = $LiCu_2{}^tBu_3(OH)^-$, b = $Li_2Cu_3{}^tBu_4(OH)_2{}^-$.

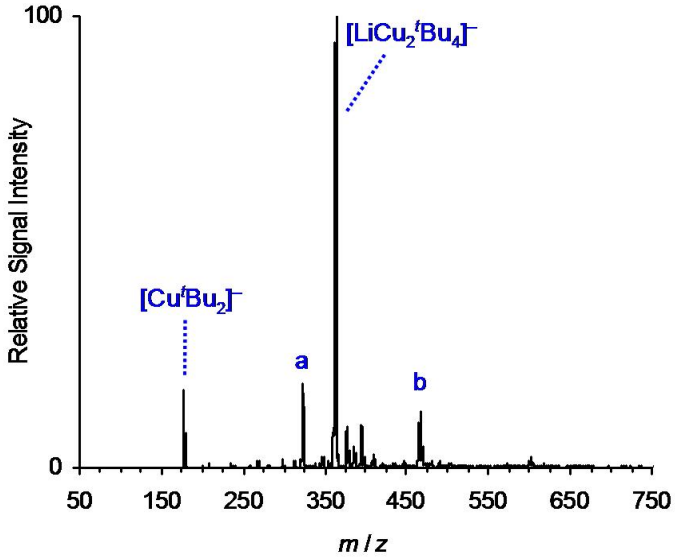

Figure S8. Negative ion mode ESI mass spectrum of a 25 mM solution of $LiCu^tBu_2 \cdot LiCN$ in MTBE, a = $LiCu_2{}^tBu_3(OH)^-$, b = $Li_2Cu_3{}^tBu_4(OH)_2{}^-$.

2.) Additional positive ion mode ESI mass spectra of $LiCuR_2$·LiCN solutions

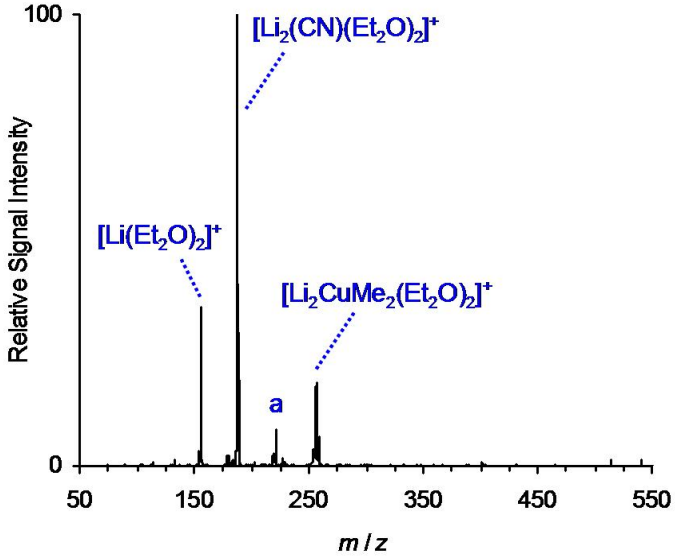

Figure S9. Positive ion mode ESI mass spectrum of a 25 mM solution of $LiCuMe_2$·LiCN in Et_2O, a = $Li_3(CN)_2(Et_2O)_2^+$.

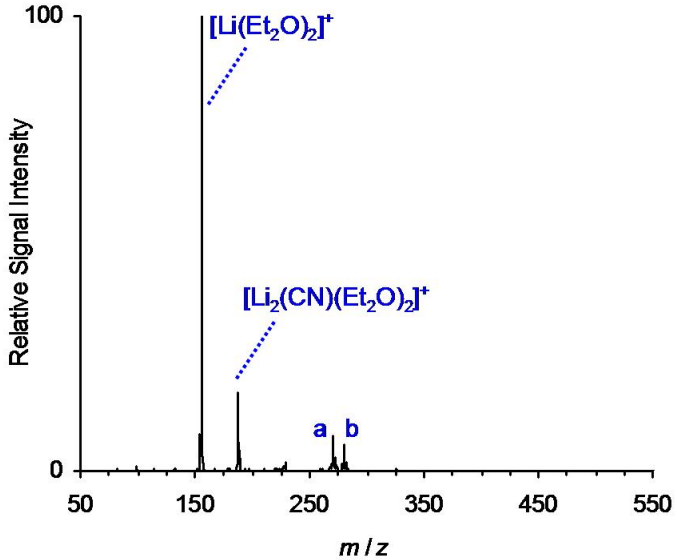

Figure S10. Positive ion mode ESI mass spectrum of a 25 mM solution of $LiCuEt_2$·LiCN in Et_2O, a = $Li_2CuEt(OH)(Et_2O)_2^+$, b = $Li_2CuEt(CN)(Et_2O)_2^+$.

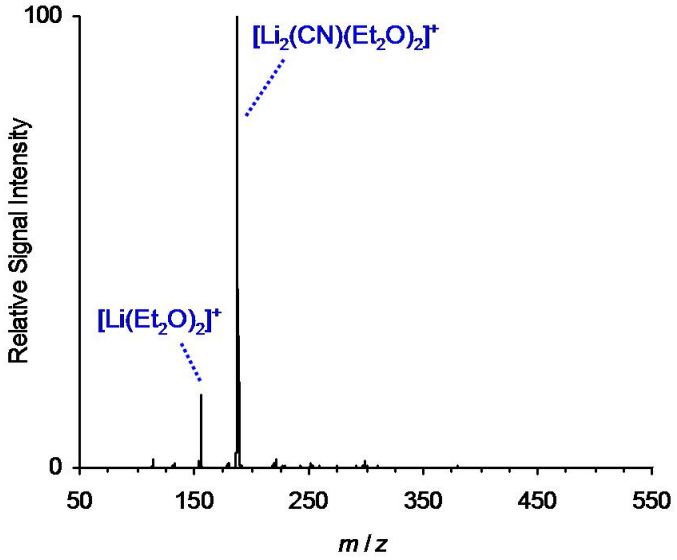

Figure S11. Positive ion mode ESI mass spectrum of a 25 mM solution of $LiCu^{n}Bu_2 \cdot LiCN$ in Et_2O.

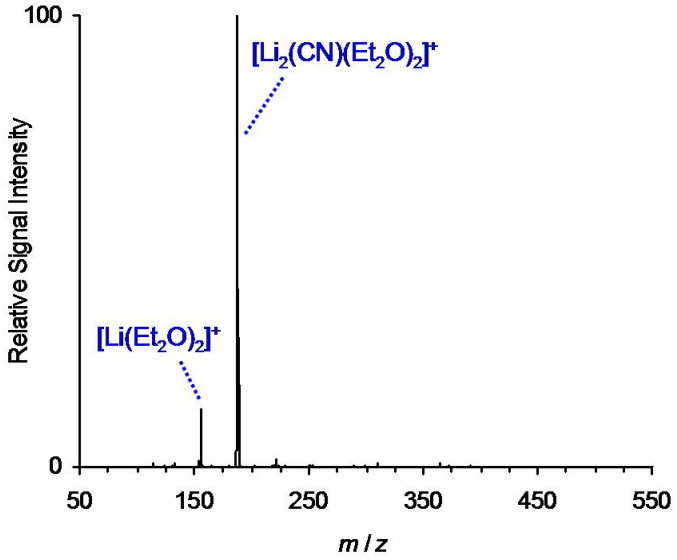

Figure S12. Positive ion mode ESI mass spectrum of a 25 mM solution of $LiCu^{s}Bu_2 \cdot LiCN$ in Et_2O.

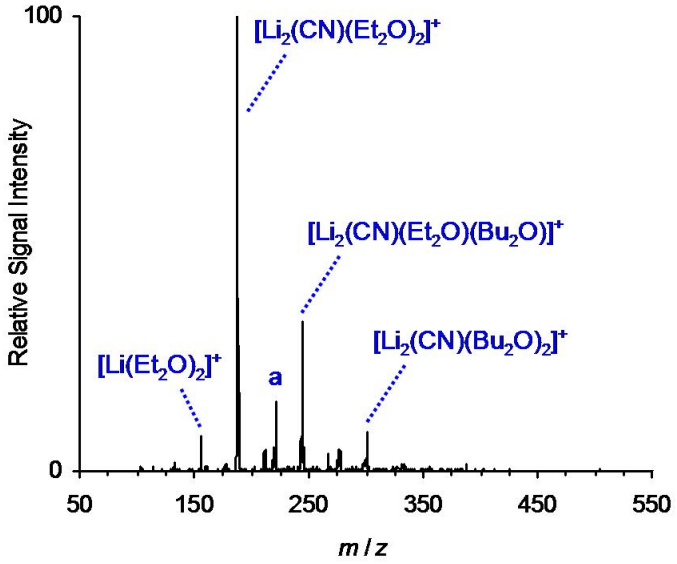

Figure S13. Positive ion mode ESI mass spectrum of a 25 mM solution of $LiCuPh_2 \cdot LiCN$ in Et_2O, a = $Li_3(CN)_2(Et_2O)_2^+$.

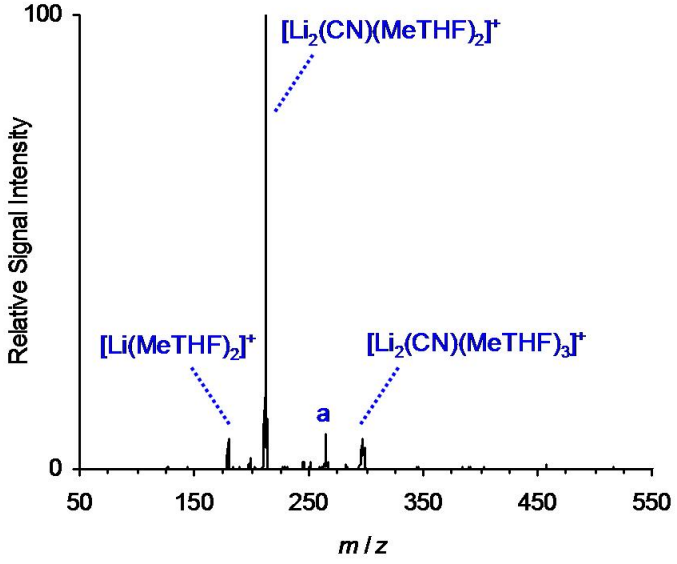

Figure S14. Positive ion mode ESI mass spectrum of a 25 mM solution of $LiCu^tBu_2 \cdot LiCN$ in MeTHF, a = $Li(MeTHF)_3^+$.

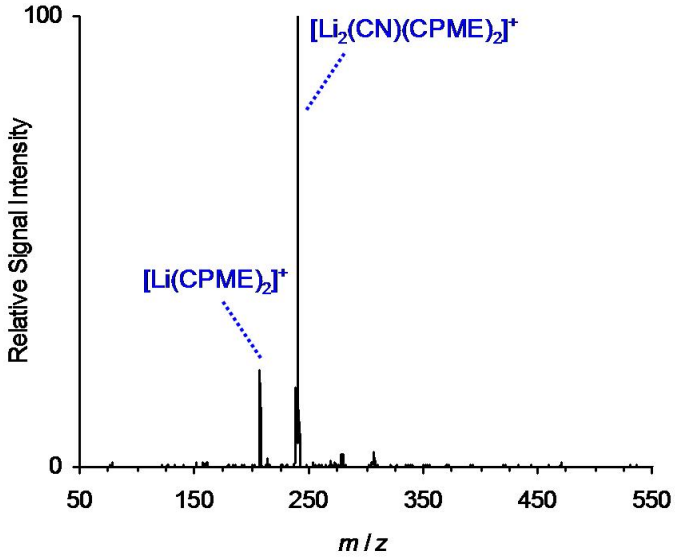

Figure S15. Positive ion mode ESI mass spectrum of a 25 mM solution of LiCu^{t}Bu$_2$·LiCN in CPME.

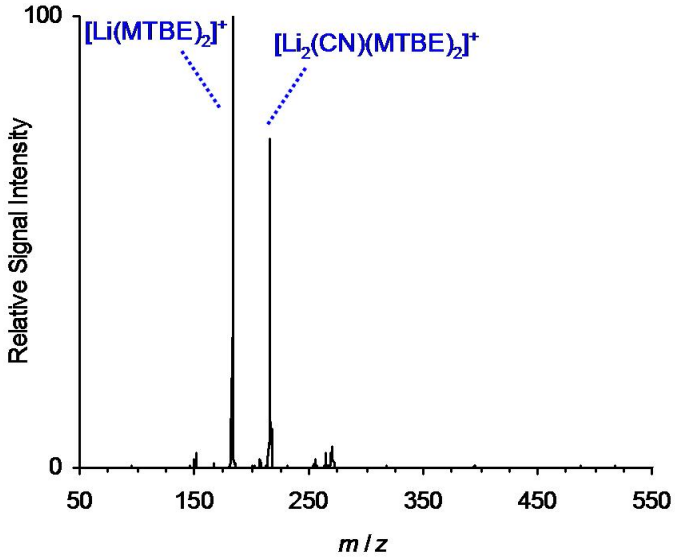

Figure S16. Positive ion mode ESI mass spectrum of a 25 mM solution of LiCu^{t}Bu$_2$·LiCN in MTBE.

3.) Additional negative ion mode ESI mass spectra of $Li_{0.8}CuR_{0.8}(CN)$ solutions

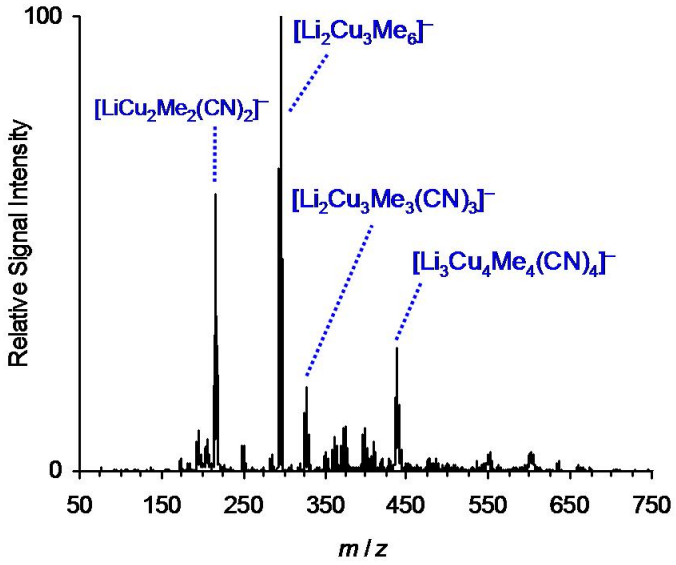

Figure S17. Negative ion mode ESI mass spectrum of a 25 mM solution of $Li_{0.8}CuMe_{0.8}(CN)$ in Et_2O.

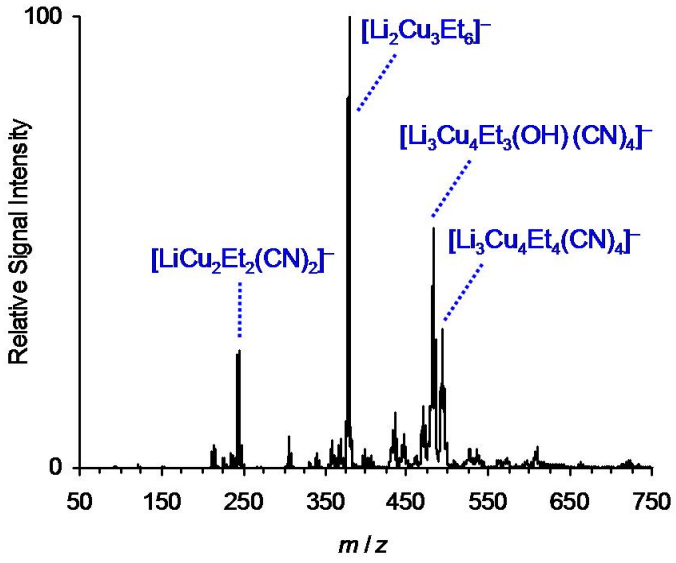

Figure S18. Negative ion mode ESI mass spectrum of a 25 mM solution of $Li_{0.8}CuEt_{0.8}(CN)$ in Et_2O.

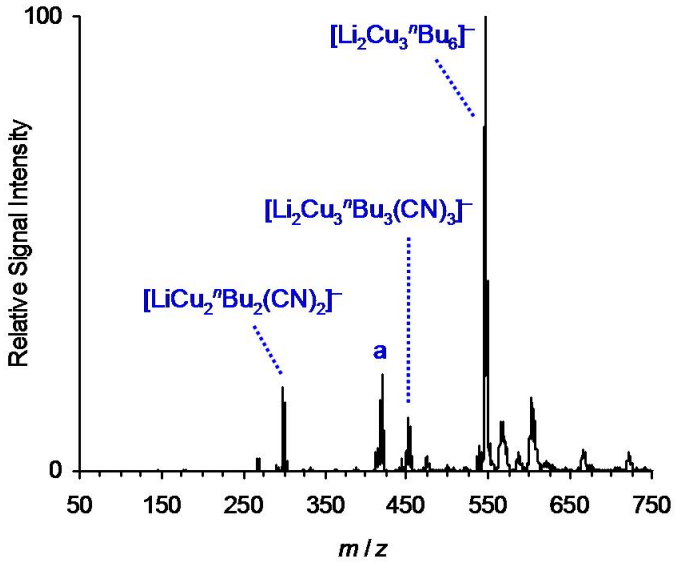

Figure S19. Negative ion mode ESI mass spectrum of a 25 mM solution of $Li_{0.8}Cu^{n}Bu_{0.8}(CN)$ in Et_2O, a = $Cu_3{}^{n}Bu_4^-$.

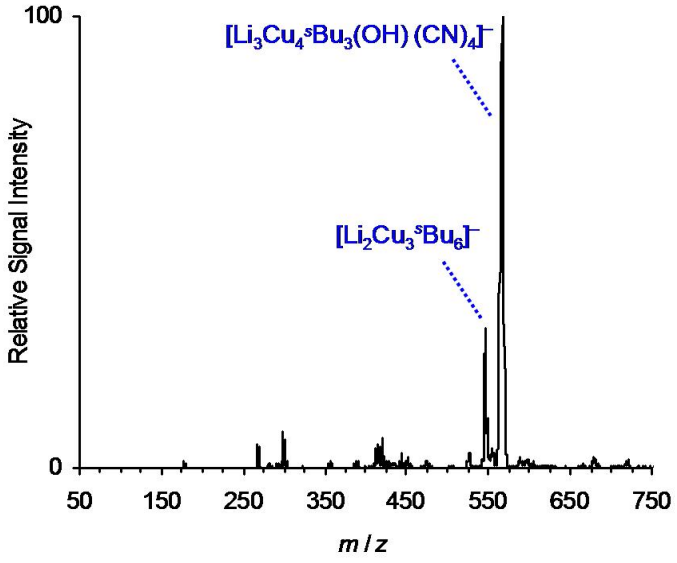

Figure S20. Negative ion mode ESI mass spectrum of a 25 mM solution of $Li_{0.8}Cu^{s}Bu_{0.8}(CN)$ in Et_2O.

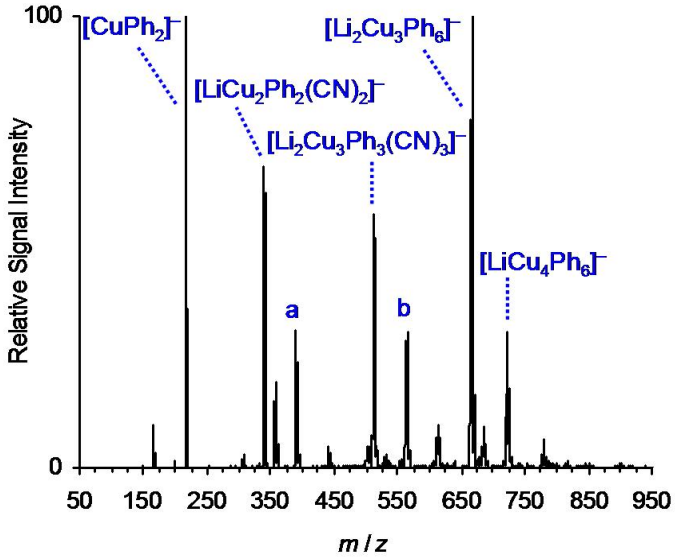

Figure S21. Negative ion mode ESI mass spectrum of a 25 mM solution of $Li_{0.8}CuPh_{0.8}(CN)$ in Et_2O, a = $LiCu_2Ph_3(CN)^-$, b = $Li_2Cu_3Ph_4(CN)_2^-$.

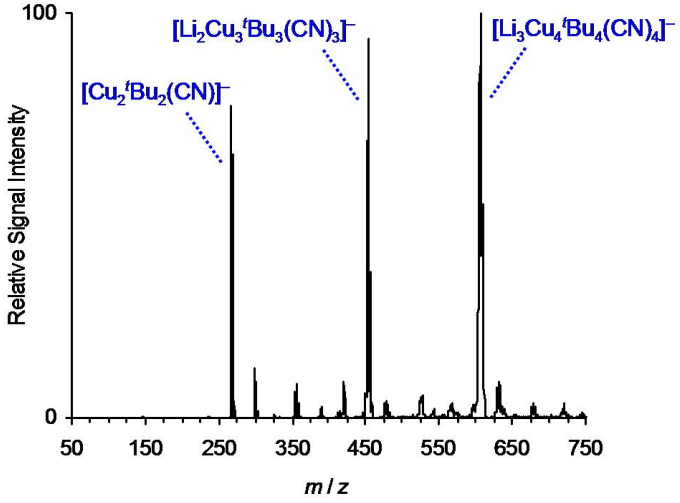

Figure S22. Negative ion mode ESI mass spectrum of a 25 mM solution of $Li_{0.8}Cu^tBu_{0.8}(CN)$ in MeTHF.

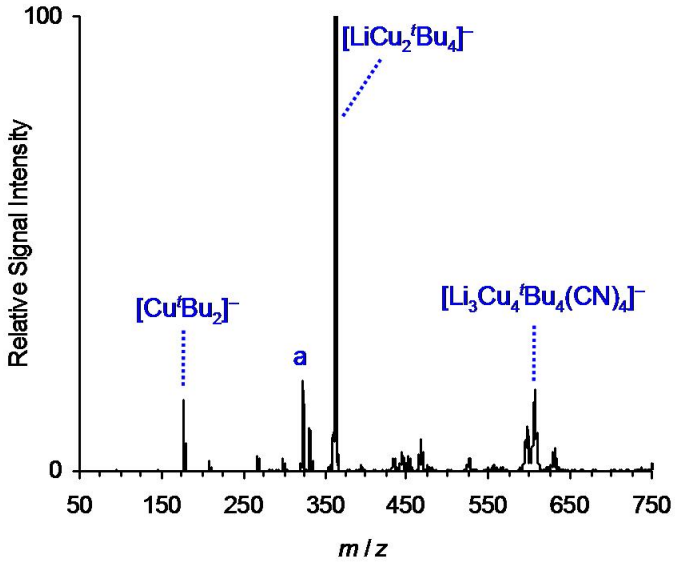

Figure S23. Negative ion mode ESI mass spectrum of a 25 mM solution of $Li_{0.8}Cu^tBu_{0.8}(CN)$ in CPME, a = $LiCu_2{}^tBu_3(OH)^-$.

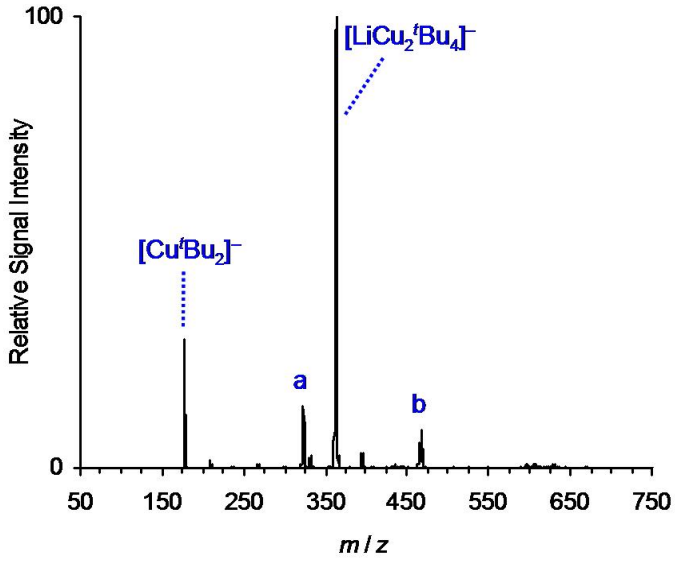

Figure S24. Negative ion mode ESI mass spectrum of a 25 mM solution of $Li_{0.8}Cu^tBu_{0.8}(CN)$ in MTBE, a = $LiCu_2{}^tBu_3(OH)^-$, b = $Li_2Cu_3{}^tBu_4(OH)_2{}^-$.

4.) Additional positive ion mode ESI mass spectra of $Li_{0.8}CuR_{0.8}(CN)$ solutions

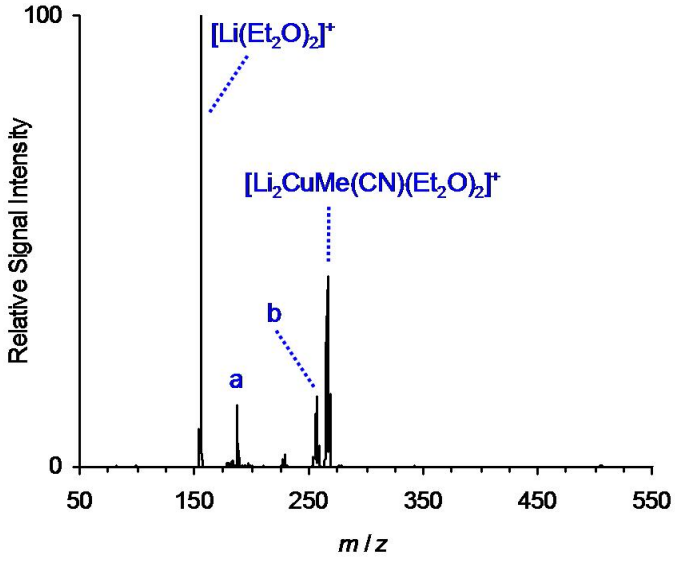

Figure S25. Positive ion mode ESI mass spectrum of a 25 mM solution of $Li_{0.8}CuMe_{0.8}(CN)$ in Et_2O, a = $Li_2(CN)(Et_2O)_2^+$, b = $Li_2CuMe_2(Et_2O)_2^+$.

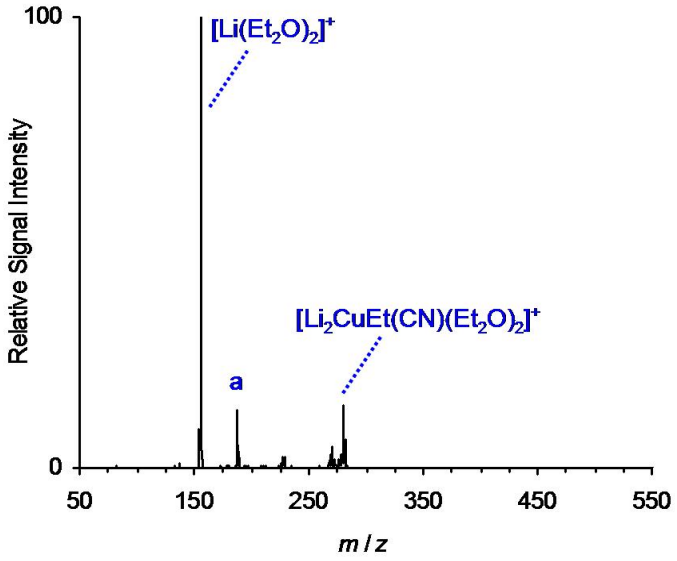

Figure S26. Positive ion mode ESI mass spectrum of a 25 mM solution of $Li_{0.8}CuEt_{0.8}(CN)$ in Et_2O, a = $Li_2(CN)(Et_2O)_2^+$.

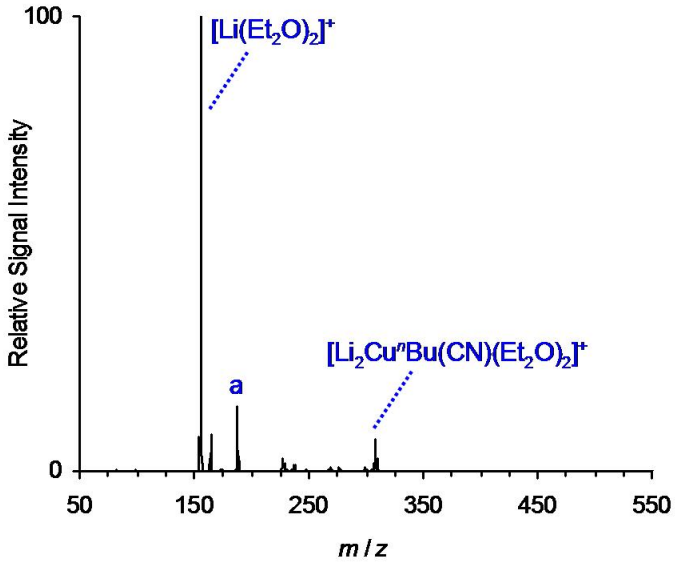

Figure S27. Positive ion mode ESI mass spectrum of a 25 mM solution of $Li_{0.8}Cu^{n}Bu_{0.8}(CN)$ in Et_2O, a = $Li_2(CN)(Et_2O)_2^+$.

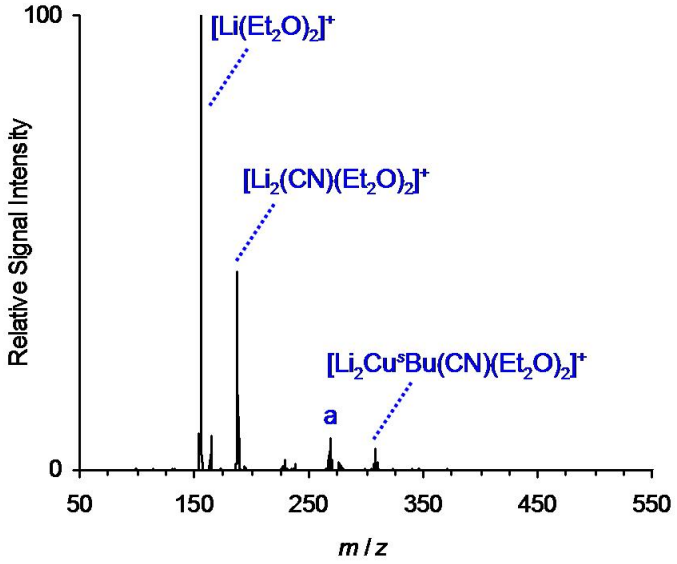

Figure S28. Positive ion mode ESI mass spectrum of a 25 mM solution of $Li_{0.8}Cu^{s}Bu_{0.8}(CN)$ in Et_2O, a = $Li_2Cu(CN)(OH)(Et_2O)_2^+$.

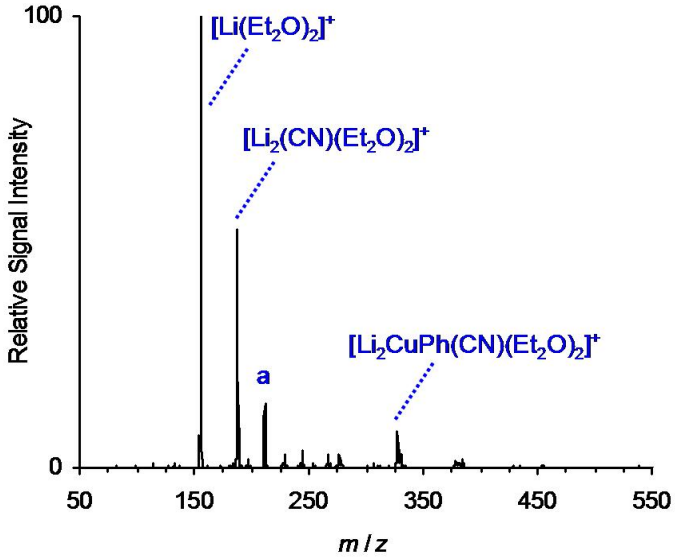

Figure S29. Positive ion mode ESI mass spectrum of a 25 mM solution of $Li_{0.8}CuPh_{0.8}(CN)$ in Et_2O, a = $Li(Et_2O)(Bu_2O)^+$.

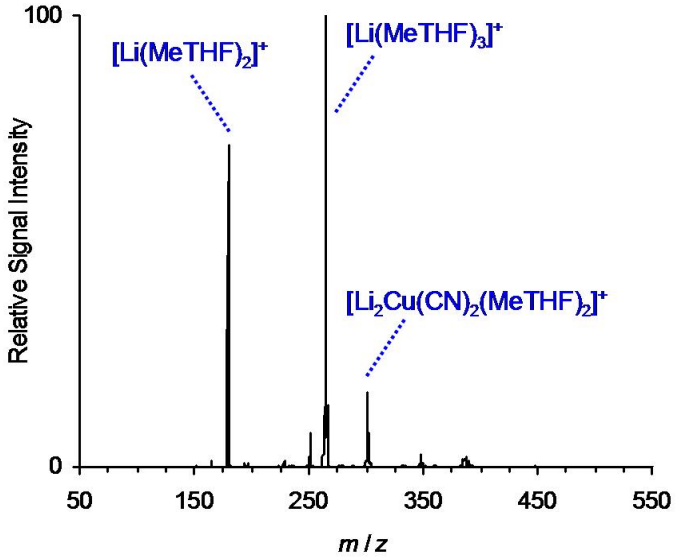

Figure S30. Positive ion mode ESI mass spectrum of a 25 mM solution of $Li_{0.8}Cu^tBu_{0.8}(CN)$ in MeTHF.

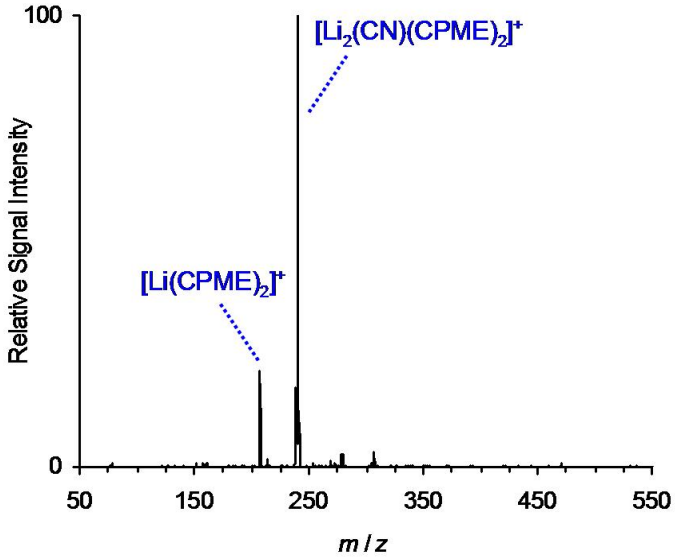

Figure S31. Positive ion mode ESI mass spectrum of a 25 mM solution of $Li_{0.8}Cu^{t}Bu_{0.8}(CN)$ in CPME.

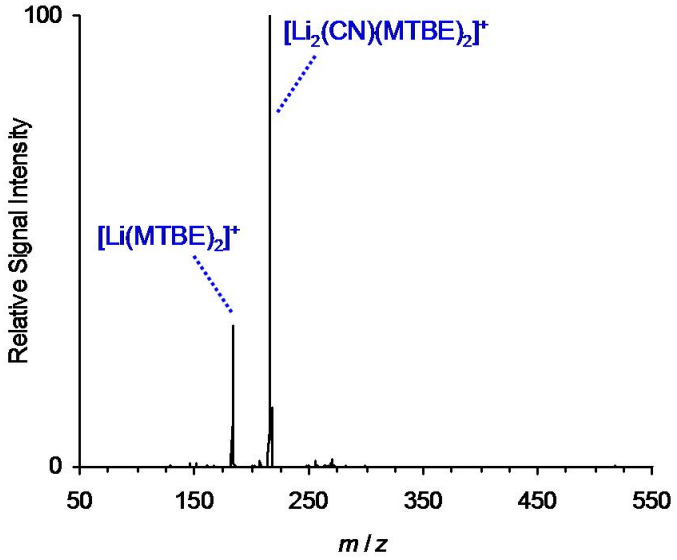

Figure S32. Positive ion mode ESI mass spectrum of a 25 mM solution of $Li_{0.8}Cu^{t}Bu_{0.8}(CN)$ in MTBE.

5.) Concentration dependence of the molar conductivity of $LiCuPh_2 \cdot LiCN$

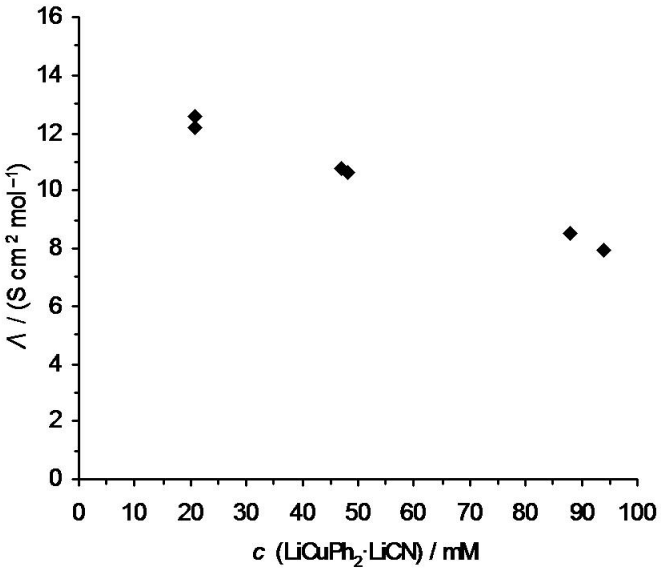

Figure S33. Concentration dependence of the molar conductivity of $LiCuPh_2 \cdot LiCN$ in THF at $T = 258$ K.

6.) Temperature dependence of the molar conductivity of LiCuPh(CN)

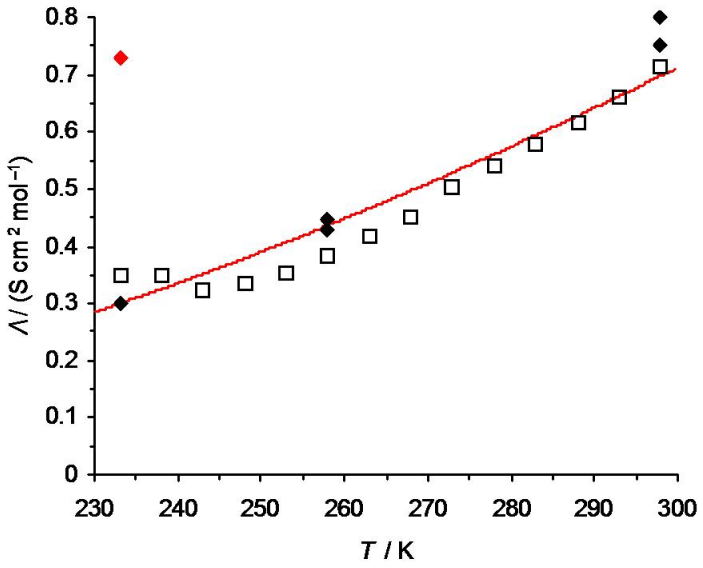

Figure S34. Temperature dependence of the molar conductivity of LiCuPh(CN) in THF, $c \approx 99$ mM. The red line corresponds to a fit that only takes into account the effect of the temperature dependence of the solvent viscosity. The open symbols represent data points collected during a single conductivity measurement, in which the temperature was raised continuously from 233 K to 298 K in 5 K increments. The filled symbols represent the data points collected independently for different samples at fixed temperatures. The filled red data point deviates significantly from the observed trend, and was not taken into account for the fitting.